small NANO MICRO

X-ray spectromicroscopy

DOI: 10.1002/smll.200500345

Chemical Mapping of Individual Semiconductor Nanostructures

*Fulvio Ratto, Andrea Locatelli, Stefano Fontana, Sharmin Kharrazi, Shriwas Ashtaputre, Sulabha K. Kulkarni, Stefan Heun, and Federico Rosei**

We demonstrate experimentally the power of a novel analytical tool for X-ray spectromicroscopy. This provides a minimally intrusive elemental mapping of surfaces at the nanoscale and holds the promise of remarkable versatility. We have applied our procedure to the characterization of Ge(Si) islands on Si(111) substrates, with the aim of investigating the surface stoichiometry gradients and gaining insight into the intermixing dynamics. By identifying Si-richer edges with respect to the centers, we are able to associate alloying in these islands to surface transport processes.

Keywords:
- atomic intermixing
- electron microscopy
- photoelectron spectroscopy
- quantum dots
- spectromicroscopy

1. Introduction

Interest in the study of nanostructured materials is driving an ever-increasing demand for experimental techniques that provide chemical information with very high spatial resolution. Most properties of various systems, ranging from semiconductors to organic/inorganic interfaces, depend on their nanoscale chemical features. Thus, the ability to probe the nanoscale spectroscopically is much needed. Existing techniques either offer a poor spatial resolution or are destructive. This is a major drawback, and therefore the development of flexible methods would represent a desirable achievement. Here we demonstrate the power of a novel procedure based on X-ray photoemission electron microscopy (XPEEM), which may be exploited for a vast range of nanostructured surfaces. We have applied our analysis to a system of great current interest in materials science, namely, the growth of self-organized Ge(Si) nanostructures. We report top-view elemental maps of individual semiconductor nanoislands with unprecedented lateral resolution (≈30 nm). The surface of single Ge(Si) nanostructures is shown to be rich in Ge at the centers and in Si at the edges, implying that intermixing is mainly due to surface transport phenomena.

Silicon surfaces with low crystallographic indices are widely used as substrates to grow Ge(Si) nanoislands.[1,2] Such nanostructures may lead to several new devices with applications in various fields, including nanoelectronics, optoelectronics, and single-electron computing.[3,4] In particular, Ge(Si) quantum dots (QDs)[5] may allow the integration of these new components with the existing Si technology. The epitaxy of Ge on Si follows the Stranski–Krastanov growth mode,[6] which arises from their 4.2% lattice mismatch. After wetting the surface up to a critical thickness of 3–5 monolayers (MLs), a roughening transition occurs via the nucleation of three-dimensional (3D) Ge(Si) islands. The process leads to a substantial release of the strain energy in the system.[7] Si/Ge atomic intermixing is another possible pathway to further reduce the mismatch strain. The average Si content within the wetting layer (WL) was mea-

[*] F. Ratto, Prof. Dr. F. Rosei
INRS Energie, Matériaux et Télécommunications
Université du Québec
1650 Boul. Lionel Boulet, J3X 1S2 Varennes (QC) (Canada)
Fax: (+1) 450-929-8102
E-mail: rosei@emt.inrs.ca
Dr. A. Locatelli, Dr. S. Fontana
Sincrotrone Trieste S.C.p.A.
S.S. 14 Km 163.5, 34012 Basovizza (Italy)
S. Kharrazi, S. Ashtaputre, Prof. Dr. S. K. Kulkarni
DST Unit on Nanoscience, Department of Physics
University of Pune, Pune 411 007 (India)
Dr. S. Heun
Laboratorio Nazionale TASC-INFM, Area Science Park
S.S. 14 Km 163.5, 34012 Basovizza (Italy)

sured to be as high as 50%,[8] whereas the stoichiometry of the emerging 3D nanoislands is poorly understood and possibly inhomogeneous at the nanoscale. Moreover, in general the alloying profile in semiconductor hetero-nanostructures identifies a critical issue in crystal growth. When embedded within the Si matrix, Ge(Si) nanostructures are expected to confine charge carriers by virtue of the local stoichiometry and strain gradients.[9,10] Thus, addressing the detailed chemical composition within individual islands would represent a great advancement. Here we demonstrate a novel technique that allows the top-view stoichiometry of the surface to be mapped with nanoscale resolution, based on XPEEM. This method has already been successfully employed in numerous specific studies, including the core levels,[11] valence band structure,[12] and size effects[13] of nanocrystals, and the spatial resolution of C hybridization states[14] or of organic molecules[15,16] (by comparison of absorption data with reference spectra). Here we propose a widely applicable method to quantify absolute atomic fractions in alloys, without any need for reference data (see the Experimental Section for details).

2. Results

Ge(Si) nanostructures were obtained by depositing ten MLs Ge on Si(111) surfaces in the temperature range 450–650 °C. After growth and quenching to room temperature, XPEEM images and spectra were acquired with a lateral and energy resolution of ≈30 nm and 0.25 eV, respectively. The surface sensitivity of the probe is of the order of the photoelectrons' escape depth, which is ≈0.5 nm in our case. This allows chemical information to be obtained from the topmost ≈0.5–2 nm of the sample's surface. Clearly resolved Ge/Si stoichiometry mapping was achieved by selecting and processing the spectra from relatively large 3D structures. The general behavior can then be inferred by scaling arguments, based on model descriptions of diffusion in ripened islands.[17,18]

Figure 1 A displays the absolute top-view surface composition map (vol% Si) of a triangular Ge(Si) 3D structure grown at 450 °C. This shape is known to correspond to a strained, coherent nanocrystal.[19] The relation between surface composition and topography can be determined by comparison with the contour plot drawn from the low-energy electron microscopy (LEEM) image reported in Figure 1 B. The stoichiometry map was obtained from the processed XPEEM micrographs in Figure 1C and D (see the Experimental Section for details). The Si concentration is highly inhomogeneous at the nanoscale, ranging from about zero in the central region of the island to as much as 10% at the edges, especially at the corners.[20] We estimate the absolute error in the measured concentrations as ±2 vol% for an acquisition time of up to two hours per spectrum.[21]

Surface chemical maps were obtained for ≈30 nanostructures grown at different deposition temperatures. Figure 2 displays an example of a chemical map obtained for a typical structure deposited at 550 °C. At island centers, the surface can contain up to ≈15% Si, which may rise monotonically to ≈40% towards the borders, depending on lateral dimensions and substrate temperature. Increasing the latter enhances surface and interlayer diffusion phenomena and lowers the density of nucleation sites, thus enlarging the average island dimensions. At the same time, intermixing is promoted as a thermally activated process. Si/Ge alloying in individual nanostructures was found to increase with deposition temperature, while preserving the qualitative inhomogeneity features described above. The Si content near the center is always somewhat depressed, though there is no clear pattern in the shape of the concentration contours, which varies considerably from island to island. By scaling considerations we also predict that the smaller nanostructures will be richer in Ge at the centers and in Si at the edges.

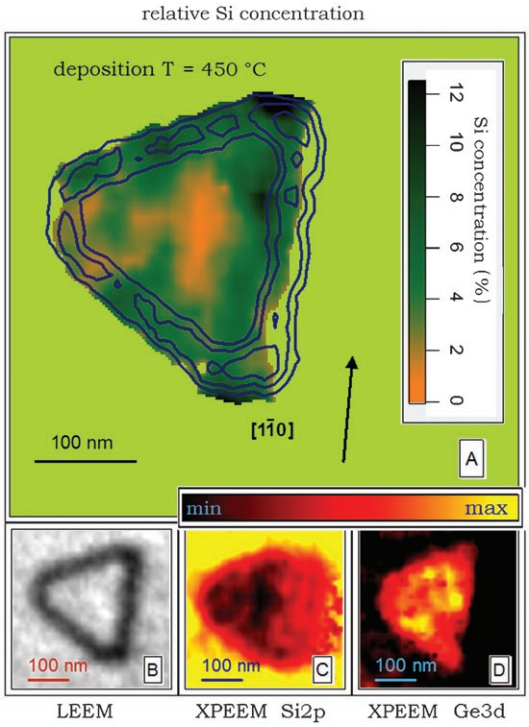

Figure 1. Typical Ge(Si) nanostructure grown at 450 °C. A) Estimated silicon surface concentration map (≈30 nm lateral resolution). The contour plot superimposed on the concentration image represents the island geometry as obtained from the electron microscopy image in (B) and serves as a guide to the eye. B) Low-energy electron microscopy (LEEM) image displaying the island-faceted topography and edge orientation along the $<1\bar{1}0>$ directions (≈10 nm lateral resolution). C) XPEEM image that results by integrating over photoelectron energies corresponding to the Si 2p core level. D) XPEEM image integrated over the Ge 3d photoelectrons. In (C) and (D), the X-ray flux impinges on the surface from left to right. In (C), the island's shadow is observed to its right. The island's height, as estimated from the shadow's length in the XPEEM micrographs, is ≈25 nm (for details, see the Experimental Section).

small NANO MICRO

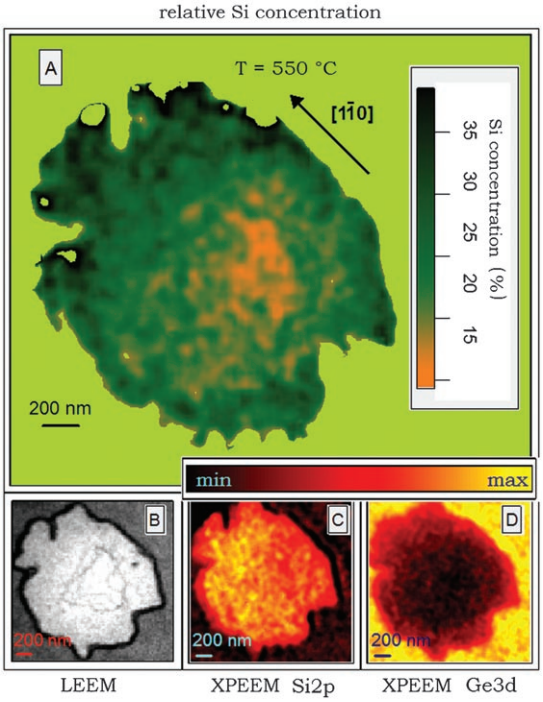

Figure 2. Absolute surface silicon content for a typical Ge(Si) ripened island grown at 550 °C. Sequence (A–D) is as in Figure 1. The Si concentration increases from 15% at the center of the island up to some 40% at the borders. The Si-depleted area tentatively corresponds to the partially eroded region visible in panel (B). This might explain a possible pathway towards the formation of atoll-like morphologies through the removal of the highly strained Ge-richer portions of the island's surface.

3. Discussion

Mapping the concentration profiles is important, among other reasons, to understand the carrier confining behavior of QDs. Their optoelectronic properties will generally depend on local chemical and strain inhomogeneities. Although the surface sensitivity of XPEEM prevents it from accessing buried layers, general considerations based on fundamental interdiffusion mechanisms allow us to infer the overall 3D stoichiometry profile. Minimization of the strain energy inside the islands and in the underlying WL may be achieved through a Si-rich island core.[22] This would occur via a flux of substrate atoms entering the 3D structures through their lower base during growth, requiring significant bulk mass exchanges. However, the thermal balance in the system may not be sufficient to activate bulk diffusion processes within the investigated temperature range. The observed stoichiometry profile matches alloying models better, based on surface transport phenomena. Highly mobile silicon atoms at the surface would diffuse throughout the WL, reach island edges, and be incorporated therein by further growth.[23] Surface-mediated incorporation would prevail over bulk exchanges, due to the relative extent of the intervening potential barriers.[24] The resulting composition profile might display Si-richer edges with respect to the cores.

The analytical technique whose results are shown here provides minimally intrusive chemical mapping,[11,25] which may be used for a wide range of sub-100-nm surface structures. This represents a substantial advantage with respect to complementary methods presently in use. Some of these suffer from poor spatial resolution (as most traditional spectroscopic tools, for example, X-ray photoemission spectroscopy). Some are considerably more destructive (e.g., cross-sectional techniques like transmission or scanning electron microscopy). Others would simply be rather impractical (e.g., energy dispersive X-ray analysis applied to scanning electron microscopy or scanning Auger microscopy would require much longer acquisition times for a comparable accuracy).[26] The surface sensitivity of XPEEM will be particularly effective in the study of nanostructured materials whose distinctive properties are determined by surface features, including, for example, nanostructured catalysts,[27] fuel-cell materials, organic/inorganic interfaces,[28,29] or biocompatible surfaces,[30] as long as the sample withstands prolonged X-ray exposure without substantial damage. Indeed this should be in general regarded as the ultimate limit of any X-ray-based technique. The power of our approach will be further enhanced by the forthcoming use of aberration-corrected optics, which ought to improve the lateral resolution of XPEEM to a few nanometers.[31,32] Immediate developments of our procedure aim at mapping the strain in high-k dielectric films (e.g. Si/Ge strained films),[33] another important challenge for the semiconductor industry in the near future.[34]

4. Conclusions

In conclusion, we have demonstrated experimentally that XPEEM can be exploited as a versatile tool to quantitatively map the chemistry of surfaces. The lateral resolution presently attains $\approx$30 nm and is soon expected to improve by about one order of magnitude. When applied to self-organized semiconductor hetero-nanostructures, our technique provides new insight on alloying dynamics. By identifying a Si content gradient pointing from the centers towards the borders of individual Ge/Si(111) nanoislands, we have associated intermixing to surface diffusion processes rather than bulk mass exchanges.

5. Experimental Section

Experiments were performed at the Nanospectroscopy beamline located at the Elettra synchrotron facility in Trieste, Italy.[35] The details for sample preparation are as follows: Si(111) substrates were cleaned in ultra-high vacuum by flash heating up to 1250 °C to remove the native oxide. This was repeated until a sharp 1 × 1 to 7 × 7 phase transition was observed while cooling down the sample.[36] Next, ten MLs of Ge were deposited at a rate of 0.2 ML min^{-1}. After growth and quenching to room temperature, the relative Ge/Si surface stoichiometry of individual

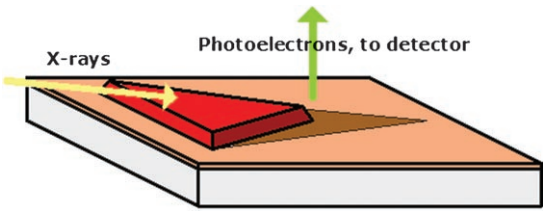

Figure 3. Scheme of a Ge(Si) nanostructure with a morphology typical of those observed on the Ge/Si(111) surface. The X-ray flux (yellow arrow) impinges the sample in a grazing configuration. Photoelectrons (green arrow) are collected from the normal direction. Outstanding features include the X-rays' shadows on specific steep facets of the islands and areas of the WL. Note however that the topmost (111)-oriented facet of the nanostructures is always completely illuminated.

nanostructures was mapped in situ using energy-filtered XPEEM. Figure 3 displays a scheme of the experimental conditions. In this illustration, a Ge(Si) island emerges from the WL and is probed by XPEEM. Photons impinge on the surface with a 16° grazing incidence angle, and photoelectrons are detected from the surface normal direction. Shadowing effects stem from the photons' grazing incidence angle and are generally accounted for while interpreting the data.[11] Nonetheless we have eluded shadows by focusing our analysis on the flat areas of the uppermost bases of the islands. The geometry of the detecting elements provides a top-view perspective on the surface.

At the selected photon energy of 130.5 eV, the Ge 3d and Si 2p photoelectron core level emissions are found at kinetic energies of ≈103 and 28 eV, respectively, which yields a ≈0.5 nm escape depth.[37] The absolute Si fraction can be evaluated by measuring and processing the overall signal stemming from the elastically scattered Ge 3d and Si 2p photoelectrons. No further physical quantities are to be estimated. Sequences of XPEEM images were acquired while scanning the photoelectron energies within ranges centered about the Ge 3d and Si 2p peaks. After background subtraction,[38] the laterally resolved Ge 3d and Si 2p spectra were integrated. This results in Ge 3d or Si 2p images of the surface whose contrast is the overall signal from the Ge 3d or Si 2p core levels. A direct comparison of these Ge 3d and Si 2p images requires proper normalization. This may be performed by dividing the spatially resolved photoelectron yields from the surface of 3D islands by those from the WL, which allows them to be disentangled from experimentally inaccessible variables.[39] Here the normalization images have been obtained by interpolating the WL intensities to underneath the 3D nanostructures. Let ι_{Ge} and ι_{Si} denote the normalized Ge 3d and Si 2p images, respectively. The average Si content C_{Si} within the topmost surface layers—that is, up to a depth of 0.5–2 nm, as defined by the 0.5-nm escape length of the photoelectrons at the observed kinetic energies—then reads:

$$C_{Si} = \frac{(\iota_{Ge} - 1)\iota_{Si}}{\iota_{Ge} - \iota_{Si}} \quad (1)$$

The details of the relevant theoretical framework have been discussed elsewhere.[40] Equation (1) relates the Si fraction in the alloy to merely experimental variables, that is, the integrated Ge 3d and Si 2p photoelectron intensities. This should be regarded as an advantage with respect to any formulation that projects a dependence of C_{Si} on quantities such as photoemission cross sections or electron escape lengths, which cannot be measured in the same experiment. Moreover, no external reference is to be used and knowledge of the detailed shape of the core level spectra is unnecessary. In particular this allows the acquisition time to be shortened considerably, which is critical to avoid or reduce damage induced by X-rays.

While individual Ge 3d and Si 2p images alone may offer an intuitive picture of the chemical inhomogeneity, a precise evaluation of the spatially resolved stoichiometry requires extreme accuracy in comparing and superimposing different sequences of images. This entails an extensive yet possible experimental endeavor, as we have demonstrated.

Acknowledgements

F. Ratto acknowledges the ICCS and FQRNT for graduate fellowships. S.K., S.A., and S.K.K. are grateful to ICTP for financial assistance. S.K.K. thanks DST and UGC India for support. F. Rosei acknowledges funding from the NSERC of Canada and salary support from FQRNT and the Canada Research Chairs program. S.K. thanks UGC India for support through a research fellowship.

[1] I. Berbezier, A. Ronda, A. Portavoce, *J. Phys. Condens. Matter* **2002**, *14*, 8283.
[2] B. Voigtländer, M. Kawamura, N. Paul, V. Cherepanov, *J. Phys. Condens. Matter* **2004**, *16*, 1535.
[3] F. Rosei, *J. Phys. Condens. Matter* **2004**, *16*, S1373.
[4] L. Oberbeck, N. J. Curson, M. Y. Simmons, R. Brenner, A. R. Hamilton, S. R. Schofield, R. G. Clark, *Appl. Phys. Lett.* **2002**, *81*, 3197.
[5] A. P. Alivisatos, *Science* **1996**, *271*, 933.
[6] Z. Zhang, M. G. Lagally, *Science* **1997**, *276*, 377.
[7] G. Medeiros-Ribeiro, A. M. Bratkovski, T. I. Kamins, D. A. A. Ohlberg, R. Stanley Williams, *Science* **1998**, *279*, 353.
[8] F. Boscherini, G. Capellini, L. Di Gaspare, F. Rosei, N. Motta, S. Mobilio, *Appl. Phys. Lett.* **2000**, *76*, 682.
[9] C. Teichert, *Phys. Rep.* **2002**, *365*, 335.
[10] P. Lever, H. H. Tan, C. Jagadish, P. Reece, M. Gal, *Appl. Phys. Lett.* **2003**, *82*, 2053.
[11] S. Heun, Y. Watanabe, B. Ressel, D. Bottomley, T. Schmidt, K. C. Prince, *Phys. Rev. B* **2001**, *63*, 125335.
[12] S. Heun, Y. Watanabe, B. Ressel, T. Schmidt, K. C. Prince, *J. Vac. Sci. Technol. B* **2001**, *19*, 2057.
[13] J. Rockenberger, F. Nolting, J. Lüning, J. Hu, A. P. Alivisatos, *J. Chem. Phys.* **2002**, *116*, 6322.
[14] C. Ziethen, F. Wegelin, G. Schönhense, R. Ohr, M. Neuhäuser, H. Hilgers, *Diamond Relat. Mater.* **2002**, *11*, 1068.
[15] C. Morin, A. P. Hitchcock, R. M. Cornelius, J. L. Brash, S. G. Urquhart, A. Scholl, A. Doran, *J. Electron Spectrosc. Relat. Phenom.* **2004**, *137–140*, 785.
[16] C. Morin, H. Ikeura–Sekiguchi, T. Tyliszczak, R. M. Cornelius, J. L. Brash, A. P. Hitchcock, A. Scholl, F. Nolting, G. Appel, D. A. Winesett, K. Kaznacheyev, H. Ade, *J. Electron Spectrosc. Relat. Phenom.* **2001**, *121*, 203.

[17] A. Malachias, S. Kycia, G. Medeiros-Ribeiro, R. Magalhães-Paniago, T. I. Kamins, R. Stanley Williams, *Phys. Rev. Lett.* **2003**, *91*, 176101.
[18] U. Denker, M. Stoffel, O. G. Schmidt, *Phys. Rev. Lett.* **2003**, *90*, 196102.
[19] N. Motta, *J. Phys. Condens. Matter* **2002**, *14*, 8353.
[20] The procedure may be less reliable at the boundaries as steep facets may determine significant variances in the local photoelectron collection efficiency.
[21] The main error sources stem from the images superposition and background subtraction procedures (see the Experimental Section and references therein) besides statistical intensity fluctuations and systematic errors. However, by analyzing flat and fully irradiated portions of the surface, away from steep edges and corners, typical sources of systematic errors are minimized. Among these, one should mention shadowing, topography, and field effects.
[22] P. Sonnet, P. C. Kelires, *Phys. Rev. B* **2002**, *66*, 205307.
[23] N. Liu, J. Tersoff, O. Baklenov, A. L. Holmes, Jr., C. K. Shih, *Phys. Rev. Lett.* **2000**, *84*, 334.
[24] R. J. Wagner, E. Gulari, *Phys. Rev. B* **2004**, *69*, 195312.
[25] C. S. Chan, G. De Stasio, S. A. Welch, M. Girasole, B. H. Frazer, M. V. Nesterova, S. Fakra, J. F. Banfield, *Science* **2004**, *303*, 1656.
[26] Scanning techniques operate in series whereas XPEEM acquires images in parallel.
[27] L. S. Byskov, J. K. Norskov, B. S. Clausen, H. Topsoe, *Catal. Lett.* **2000**, *64*, 95.
[28] M. Cavallini, F. Biscarini, S. Léon, F. Zerbetto, G. Bottari, D. A. Leigh, *Science* **2003**, *299*, 531.
[29] A. M. Jackson, J. W. Myerson, F. Stellacci, *Nat. Mater.* **2004**, *3*, 330.
[30] P. T. de Oliveira, A. Nanci, *Biomaterials* **2004**, *25*, 403.
[31] T. Schmidt, U. Groh, R. Fink, E. Umbach, O. Schaff, W. Engel, B. Richter, H. Kuhlenbeck, R. Schloegl, H. J. Freund, A. M. Bradshaw, D. Preikszas, P. Hartel, R. Spehr, H. Rose, G. Lilienkamp, E. Bauer, G. Benner, *Surf. Rev. Lett.* **2002**, *9*, 223.
[32] W. Wan, J. Feng, H. A. Padmore, D. S. Robin, *Nucl. Instrum. Methods Phys. Res. Sect. A* **2004**, *519*, 222.
[33] A. P. Hitchcock, T. Tyliszczak, P. Aebi, X. H. Feng, Z. H. Lu, J. M. Baribeau, T. E. Jackman, *Surf. Sci.* **1994**, *301*, 260.
[34] See for example, The International Technology Roadmap for Semiconductors: http://public.itrs.net/
[35] A. Locatelli, A. Bianco, D. Cocco, S. Cherifi, S. Heun, M. Marsi, M. Pasqualetto, E. Bauer, *J. Phys. IV* **2003**, *104*, 99, or see http://www.elettra.trieste.it/experiments/beamlines/nano/index.html for details on the beamline, insertion device, and end station.
[36] J. B. Hannon, F. J. Meyer zu Heringdorf, J. Tersoff, R. M. Tromp, *Phys. Rev. Lett.* **2001**, *86*, 4871.
[37] S. Tanuma, C. J. Powell, D. R. Penn, *Surf. Interface Anal.* **1991**, *17*, 911.
[38] Here the background has been modelled with a double-exponential analytical form. This was used for fitting the tails of the measured Ge 3d and Si 2p spectra separately, thus providing an estimate of the background intensity at the Ge 3d and Si 2p photoelectron energies separately.
[39] Among these are factors inherent to the system (e.g. the photoemission cross sections) and to the experimental setup (e.g. the local X-ray flux density).
[40] F. Ratto, F. Rosei, A. Locatelli, S. Cherifi, S. Fontana, S. Heun, P. D. Szkutnik, A. Sgarlata, M. De Crescenzi, N. Motta, *J. Appl. Phys.* **2005**, *97*, 043516.

Received: September 16, 2005
Revised: October 25, 2005

